Available online at www.sciencedirect.com
SCIENCE DIRECT
Nuclear Engineering and Design 236 (2006) 1800–1809
Nuclear Engineering and Design
www.elsevier.com/locate/nucengdes

A generalized flow correlation for two-phase natural circulation loops

M.R. Gartia, P.K. Vijayan *, D.S. Pilkhwal

Reactor Engineering Division, Bhabha Atomic Research Centre, Trombay, Mumbai 400085, India

Received 10 October 2005; received in revised form 2 February 2006; accepted 2 February 2006

Abstract

A generalized correlation has been proposed to estimate the steady-state flow in two-phase natural circulation loops. The steady-state governing equations for homogeneous equilibrium model, viz. continuity, momentum and energy equations have been solved to obtain the dimensionless flow rate as a function of a modified Grashof number and a geometric number. To establish the validity of this correlation, two-phase natural circulation flow rate data from five different loops have been tested with the proposed correlation and found to be in good agreement.

1. Introduction

Two-phase natural circulation is capable of generating larger buoyancy forces and hence larger flows. Two-phase natural circulation finds application in nuclear steam generators, thermosyphon boilers, boilers in fossil fuelled power plants, reactor core cooling, etc. The heat transport capabilities of natural circulation loops depend on the flow rate it can generate. For two-phase natural circulation loops, explicit correlations for steady-state flow are not available. This makes it difficult to compare the performance of different two-phase natural circulation loops. Therefore, we present an analytical correlation for steady-state flow, which is then non-dimensionalized to obtain a generalized correlation. This generalized correlation has been tested against data generated in five test facilities differing in diameter.

Pioneering work in the field of scaling laws for nuclear reactor systems have been carried out by Nahavandi et al. (1979), Zuber (1980), Heisler (1982), Ishii and Kataoka (1984), Kocamustafaogullari and Ishii (1987), Schwartzbeck and Kocamustafaogullari (1989), Yadigaroglu and Zeller (1994), Reyes Jr. (1994) and Vijayan et al. (1999). The scaling law proposed by Zuber (1980) is also known as the power-to-volume scaling philosophy. The integral test facility being set-up to simulate the advanced heavy water reactor (AHWR) has been designed based on this philosophy. However, the power-to-volume scaling philosophy has certain inherent distortions (especially in downsized components), which can suppress certain natural circulation specific phenomena like the instability (Nayak et al., 1998). Scaling laws provided by Ishii and Kataoka (1984) had been widely used for two-phase natural circulation loops. The PUMA facility simulating the simplified boiling water reactor (SBWR) has been designed based on this philosophy. Kocamustafaogullari and Ishii (1987) have given a scaling law for two-phase flow transients using reduced pressure Freon (R-11 or R-113) systems. A flow pattern transition-dependent scaling law has been given by Schwartzbeck and Kocamustafaogullari (1989). Yadigaroglu and Zeller (1994) had given a fluid-to-fluid scaling law for gravity and flashing driven natural circulation loop. Reyes Jr. (1994) has applied catastrophe functions to describe the scaling for two-phase natural circulation loops. One of the problems associated with these scaling laws is that the numbers of similarity groups are too many and they do not provide steady state or stability solutions in terms of the proposed similarity groups. Therefore, testing of these scaling laws with the available experimental data is rather difficult without the use of system codes. This arises due to the fact that more than one scaling parameter is a function of the flow rate, which for a natural circulation loop is not known a priori.

To overcome this problem, Vijayan et al. (2000) proposed a scaling procedure by which the steady-state flow rate can be obtained as a function of just one similarity group for uniform diameter loops with adiabatic pipes operating without any sub-cooling. But the proposed correlation had not been tested rigorously. In the present paper, a generalized scaling philosophy has been proposed for two-phase natural circulation loops.

* Corresponding author. Tel.: +91 22 2559 5157; fax: +91 22 2550 5151.
E-mail address: vijayanp@apsara.barc.ernet.in (P.K. Vijayan).

0029-5493/$ – see front matter © 2006 Elsevier B.V. All rights reserved.
doi:10.1016/j.nucengdes.2006.02.004

Nomenclature

General symbols

a	dimensionless flow area (A/A_r)
A	flow area (m^2)
b	constant in Eq. (7)
c_p	specific heat (J/kg K)
d	dimensionless hydraulic diameter
D	hydraulic diameter (m)
f	Darcy–Weisbach friction factor
g	gravitational acceleration (m/s^2)
Gr_m	modified Grashof number
h	enthalpy (J/kg)
h_{fg}	latent heat, $h_g - h_l$ (J/kg)
H	loop height (m)
$\mathcal{H}$	dimensionless enthalpy
k	thermal conductivity (W/m K)
K	local pressure loss coefficient
l	dimensionless length (L_i/L_t)
L	length (m)
N	total number of pipe segments
N_G	dimensionless parameter defined by Eq. (10)
p	constant in Eq. (7)
P	pressure (N/m^2)
q''	heat flux (W/m^2)
Q	total heat input rate (W)
Re	Reynolds number ($DW/A\mu$)
s	co-ordinate around the loop (m)
S	dimensionless co-ordinate around the loop (s/H)
t	time (s)
T	temperature (K)
v	specific volume (m^3/kg)
v_{fg}	$v_g = v_l$ (m^3/kg)
V_t	total loop volume (m^3)
W	mass flow rate (kg/s)
x	exit quality
z	elevation (m)
Z	dimensionless elevation (z/H)

Greek letters

α	void fraction
β_{tp}	two-phase thermal expansion coefficient (kg/J)
ϕ^2_{LO}	two-phase friction multiplier
$\bar{\phi}^2_{LO}$	average two-phase friction multiplier
μ	dynamic viscosity (N s/m^2)
ρ	density (kg/m^3)
ρ_{fg}	$\rho_g - \rho_l$ (kg/m^3)
ρ_r	reference density (kg/m^3)
τ	dimensionless time
ω	dimensionless mass flow rate

Subscripts

c	cooler
eff	effective
eq	equivalent
g	vapor
h	heater
he	heater exit
i	ith segment
in	inlet
l	liquid
LO	liquid only
m	mean
out	outlet
p	pipe
r	reference value
sp	single-phase
ss	steady state
t	total
tp	two-phase

This has been derived in the same line as that of Vijayan et al. (2000). The similarity parameter has been tested against the available data on steady-state flow. This exercise has shown that the steady-state behaviour of two-phase natural circulation loops can be simulated by a single-dimensionless parameter.

2. Steady-state behavior of two-phase natural circulation loops

The theoretical development described below is based on homogeneous equilibrium model and valid for both uniform as well as non-uniform diameter natural circulation loops. Schematic of two typical uniform diameter natural circulation loops are shown in Fig. 1. The following assumptions are made in the theoretical development:

1. Heat losses in the piping are negligible.
2. Complete separation of steam and water is assumed to occur in the steam drum (SD) so that there is no liquid carryover with the steam and no vapor carry-under with water.
3. A constant level is maintained in the SD, so that the single-phase lines always run full.
4. The heater is supplied with a uniform heat flux and the SD can be approximated to a point heat sink.

2.1. Governing equations

The one-dimensional steady-state Navier–Stokes equations for two-phase natural circulation system can be written as follows:

$$\text{continuity equation}: \quad \frac{\mathrm{d}}{\mathrm{d}s}\left(\frac{W}{A}\right) = 0 \tag{1}$$

$$\text{energy equation}: \quad \frac{W}{A}\frac{\mathrm{d}h}{\mathrm{d}s} = \begin{cases} \dfrac{4q''_h}{D_h} & \text{heater} \\ 0 & \text{adiabatic pipes} \\ -\dfrac{4q''_c}{D_c} & \text{cooler} \end{cases} \tag{2}$$

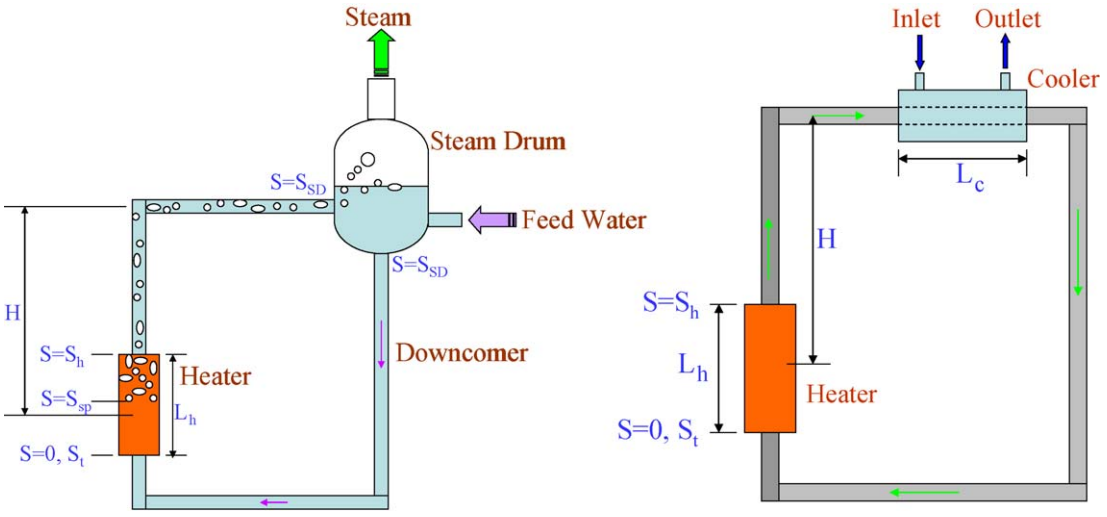

Fig. 1. Schematic of uniform diameter natural circulation loops.

$$\text{momentum equation}: \quad \frac{W^2}{A^2}\frac{\mathrm{d}}{\mathrm{d}s}\left(\frac{1}{\rho}\right) = -\frac{\mathrm{d}P}{\mathrm{d}s} - \rho g \sin\theta - \frac{fW^2}{2D\rho A^2} - \frac{KW^2}{2\rho A^2 L_\mathrm{t}} \tag{3}$$

where θ is the angle with the horizontal in the direction of flow. The second term on the right-hand side of Eq. (3) represents the body force per unit volume whereas the third and fourth terms, respectively, represent the distributed and the local friction forces per unit volume. Noting that $v = 1/\rho$ integrating the momentum equation around the circulation loop

$$\frac{W^2}{A^2}\oint \mathrm{d}v = -\oint \mathrm{d}P - g\oint \rho\,\mathrm{d}z - \frac{fW^2 L_\mathrm{t}}{2D\rho A^2} - \frac{KW^2}{2\rho A^2} \tag{4}$$

where $\mathrm{d}z = \mathrm{d}s\sin\theta$

Noting that $\oint \mathrm{d}v = 0$ and $\oint \mathrm{d}P = 0$ for a closed loop, we can write

$$0 = -g\oint \rho\,\mathrm{d}z - \frac{fW^2 L_\mathrm{t}}{2D\rho A^2} - \frac{KW^2}{2\rho A^2} \tag{5}$$

In the two-phase regions, the density is assumed to vary as $\rho_\mathrm{tp} = \rho_\mathrm{r}[1 - \beta_\mathrm{tp}(h - h_\mathrm{r})]$ in the buoyancy force term. For the estimation of frictional pressure loss, liquid density ρ_l is used in single-phase regions and the two-phase density ρ_tp is used in the riser. For the heater, an average density ρ_m is used. With these and the two-phase friction factor multiplier ϕ^2_LO, Eq. (5) can be rewritten as

$$0 = g\rho_\mathrm{r}\beta_\mathrm{tp}\oint h\,\mathrm{d}z - \sum_{i=1}^{N_\mathrm{sp}}\left(\frac{fL_\mathrm{eff}}{D}\right)_{i,\mathrm{sp}} \times \frac{W_i^2}{\rho_\mathrm{l}A_i^2} + \bar{\phi}^2_\mathrm{LO}\sum_{i=N_\mathrm{sp}}^{N_\mathrm{he}}\left(\frac{fL_\mathrm{eff}}{D}\right)_{i,\mathrm{sp}}\frac{W_i^2}{\rho_\mathrm{l}A_i^2} + \phi^2_\mathrm{LO}\sum_{i=N_\mathrm{he}}^{N_\mathrm{t}}\left(\frac{fL_\mathrm{eff}}{D}\right)_{i,\mathrm{sp}}\frac{W_i^2}{\rho_\mathrm{l}A_i^2} \tag{6}$$

Now the above equations can be non-dimensionalized using the following substitutions:

$$\omega = \frac{W}{W_\mathrm{ss}}, \quad \mathcal{H} = \frac{h - h_\mathrm{r}}{(\Delta h)_\mathrm{ss}}, \quad Z = \frac{z}{H}, \quad S = \frac{s}{H},$$

$$a_i = \frac{A_i}{A_\mathrm{r}}, \quad d_i = \frac{D_i}{D_\mathrm{r}}, \quad l_i = \frac{L_i}{L_\mathrm{t}}$$

$$A_\mathrm{r} = \frac{\sum_{i=1}^{N} A_i L_i}{\sum L_i} = \frac{V_\mathrm{t}}{L_\mathrm{t}}, \quad D_\mathrm{r} = \frac{\sum_{i=1}^{N} D_i L_i}{L_\mathrm{t}},$$

$$(l_\mathrm{eff})_i = \frac{(L_\mathrm{eff})_i}{L_\mathrm{t}}, \quad \rho_\mathrm{r} = \rho_\mathrm{in}, \quad h_\mathrm{r} = h_\mathrm{in}$$

$$f_i = \frac{p}{Re_i^b} = \frac{p}{Re_\mathrm{ss}^b}\frac{\omega^{-b}a_i^b\mu_i^b}{d_i^b\mu_\mathrm{r}^b}, \quad Re_\mathrm{ss} = \frac{D_\mathrm{r}W_\mathrm{ss}}{A_\mathrm{r}\mu_\mathrm{r}} \quad \text{and}$$

$$L_\mathrm{eff} = L_i + L_\mathrm{eq}, \quad \mu_\mathrm{r} = \frac{\sum_i \mu_i L_i}{\sum_i L_i} \tag{7}$$

At steady state, putting $\omega = W/W_\mathrm{ss} = 1$, $\mu_i = \mu_\mathrm{r}$ and $q_\mathrm{c} = q_\mathrm{h}$ the non-dimensional equations will become

$$\frac{\mathrm{d}}{\mathrm{d}S}\left(\frac{\omega}{a}\right) = 0 \tag{8}$$

$$0 = \frac{g\rho_\mathrm{r}\beta_\mathrm{tp}H(\Delta h)_\mathrm{ss}A_\mathrm{r}V_\mathrm{t}\rho_\mathrm{r}}{L_\mathrm{t}W_\mathrm{ss}^2}\oint \mathcal{H}\,\mathrm{d}Z - \frac{p}{2}\frac{Re_\mathrm{ss}^{2-b}\mu_\mathrm{r}^2}{D_\mathrm{r}^2\rho_\mathrm{l}}\frac{A_\mathrm{r}V_\mathrm{t}\rho_\mathrm{r}}{L_\mathrm{t}W_\mathrm{ss}^2}N_\mathrm{G} \tag{9}$$

where

$$N_\mathrm{G} = \frac{L_\mathrm{t}}{D_\mathrm{r}}\left[\sum_{i=1}^{N_\mathrm{sp}}\frac{(l_\mathrm{eff})_i}{d_i^{1+b}a_i^{2-b}} + \bar{\phi}^2_\mathrm{LO}\sum_{i=N_\mathrm{sp}}^{N_\mathrm{he}}\frac{(l_\mathrm{eff})_i}{d_i^{1+b}a_i^{2-b}} + \phi^2_\mathrm{LO}\sum_{i=N_\mathrm{he}}^{N_\mathrm{t}}\frac{(l_\mathrm{eff})_i}{d_i^{1+b}a_i^{2-b}}\right] \tag{10}$$

It may be noted that for uniform diameter loop, N_G reduces to the following equation:

$$N_G = \frac{L_t}{D_r}[(l_{eff})_{sp} + \bar{\phi}^2_{LO}(l_{eff})^{he}_{sp} + \phi^2_{LO}(l_{eff})^{t}_{he}] \tag{11}$$

$$\frac{d\mathcal{H}}{dS} = \phi_h \frac{V_t}{V_h}, \quad \text{where } \phi_h = a_h \frac{H}{L_t} \tag{12}$$

$$\frac{d\mathcal{H}}{dS} = -\phi_c \frac{V_t}{V_c}, \quad \text{where } \phi_c = a_c \frac{H}{L_t} \tag{13}$$

After applying the boundary conditions for the heater (at the inlet of heater $\mathcal{H} = \mathcal{H}_{in}$ and at the outlet of the heater $\mathcal{H} = \mathcal{H}_{out}$) and for the cooler section (at the cooler inlet $\mathcal{H} = \mathcal{H}_{out}$ and at the cooler outlet $\mathcal{H} = \mathcal{H}_{in}$), it can be shown that $\oint \mathcal{H}\, dZ = 1$. Hence,

$$W_{ss} = \left[\frac{2}{p}\frac{g\rho_r\beta_{tp}HQD^b_r A^{2-b}_r \rho_l}{\mu^b_r N_G}\right]^{1/3-b} \tag{14}$$

$$Re_{ss} = 0.176776\left(\frac{Gr_m}{N_G}\right)^{0.5} : \quad \text{laminar flow} \tag{15}$$

$$Re_{ss} = 1.9561\left(\frac{Gr_m}{N_G}\right)^{0.36364} : \quad \text{turbulent flow} \tag{16}$$

where

$$Gr_m = \frac{D^3_r \rho_r \rho_l \beta_{tp} g HQ}{A_r \mu^3_r}$$

2.2. Estimation of β_{tp}

We have proposed a new parameter, β_{tp}, which is the two-phase thermal expansion coefficient. We have assumed a linear variation of density inside the heater. Hence, to check the accuracy of this assumption, the density has been calculated for various pressure levels and qualities. It was found that beyond a quality of about 0.1 (10%), the two-phase thermal expansion coefficient is practically a constant for all pressure levels and its value is the same, independent of pressure and quality as shown in Fig. 2.

β_{tp} in terms of densities can be calculated using the relation

$$\beta_{tp} = \frac{1}{v}\left(\frac{\partial v}{\partial h}\right)_P = \frac{1}{(v_{in} + v_{exit})/2}\left(\frac{v_{exit} - v_{in}}{h_{exit} - h_{in}}\right)$$
$$= \frac{\rho_{in} - \rho_{exit}}{((\rho_{exit} + \rho_{in})/2)\,\Delta h} \tag{17a}$$

2.3. Special cases for β_{tp}

In Eqs. (6) and (9), β_{tp} has been considered to be constant and is approximated by a mean value over the whole loop given by Eq. (17a). In reality, β_{tp} varies as shown in Fig. 2 for water. That is, if we will not take β_{tp} as a constant, then the integral can be represented by

$$\beta_I = \oint \beta_{tp}\mathcal{H}\, dZ \tag{17b}$$

So, one can numerically integrate the above equation to obtain a more accurate prediction. But, this way one would loose the simplicity of Eq. (14). The other possible calculation of β_{tp} may be

i. $\beta_{tp} = \frac{1}{v}\left(\frac{\partial v}{\partial h}\right)_P$ and calculation of v is based on exit quality, x_{exit}. (17c)

ii. Calculation of v is based on half the value of exit quality, $\frac{1}{2}x_{exit}$. (17d)

iii. Inside the heater calculation of v is based on half the value of exit quality and in the riser portion it is based on the exit quality. (17e)

A comparison has been made while calculating the mass flow rate considering the above special cases of β_{tp} and is shown in Fig. 3.

2.4. Estimation of ϕ^2_{LO}

The mean value of ϕ^2_{LO} has been used over the heated section. Since quality variation is linear for the uniformly heated test section, $\bar{\phi}^2_{LO}$ can be evaluated at half the value of the exit quality. From the basic definition of ϕ^2_{LO} and McAdam's model for two-phase viscosity, the equations for ϕ^2_{LO} and $\bar{\phi}^2_{LO}$ can be obtained as follows:

$$\phi^2_{LO} = \frac{\rho_l}{\rho_{exit}}\left[\frac{1}{1 + x((\mu_l/\mu_g) - 1)}\right]^b \quad \text{and}$$
$$\bar{\phi}^2_{LO} = \frac{\rho_l}{\bar{\rho}_{exit}}\left[\frac{1}{1 + (x/2)((\mu_l/\mu_g) - 1)}\right]^b \tag{18}$$

where

$$\rho_{exit} = \frac{\rho_g \rho_l}{x(\rho_l - \rho_g) + \rho_g}$$

and

$$\bar{\rho}_{exit} = \frac{\rho_g \rho_l}{(x/2)(\rho_l - \rho_g) + \rho_g}$$

There are several others two-phase friction multiplier correlations available in the literature and one could choose any one of these (IAEA-TECDOC-1203).

2.5. Estimation of h_{in}

The enthalpy at the inlet of the heated section is calculated by a static energy balance at the steam drum assuming complete separation. The separated water mixes with the feed water

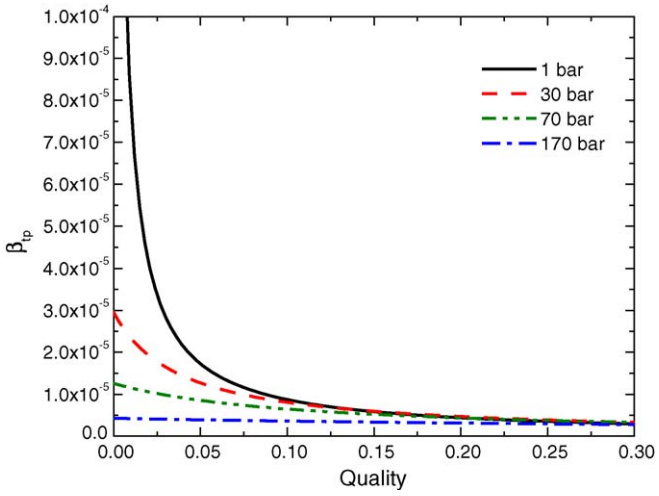

Fig. 2. Variation of β_{tp} with pressure and quality.

and the mix mean enthalpy is obtained by an energy balance as below:

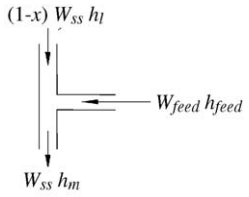

At the mixing section of the SD

$$W_{ss}(1-x)h_l + W_{feed}h_{feed} = W_{ss}h_m$$

Under steady-state condition, $W_{feed} = W_{ss}x$. Using this and noting that $h_m = h_{in}$ under steady-state condition, we obtain

$$h_{in} = h_l + x(h_{feed} - h_l)$$

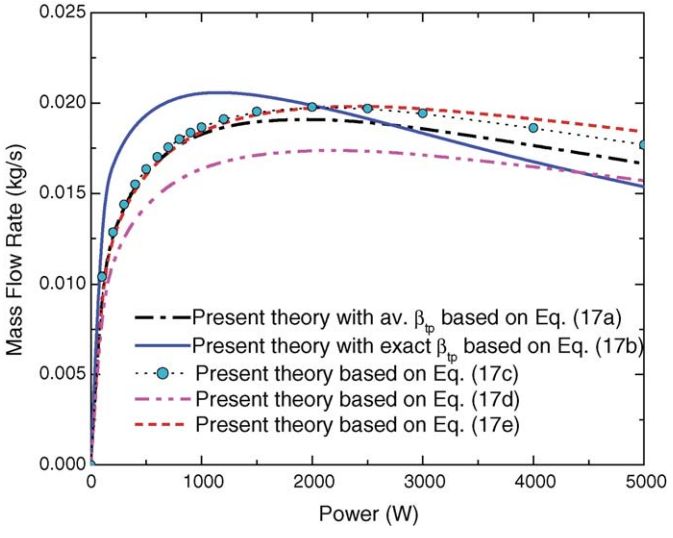

Fig. 3. Prediction of mass flow rate using different models for two-phase thermal expansion coefficient.

2.6. Estimation of ρ_{in}

$$W(1-x)c_pT_{sat} + Wxc_pT_{feed} = Wc_pT_{in}$$

$$T_{in} = T_{sat} + x(T_{feed} - T_{sat})$$

Now knowing the system pressure, p and the inlet temperature, T_{in} the inlet density ρ_{in} can be calculated.

3. Experimental validation

3.1. Experimental loop

To validate the above proposition, an experimental facility was constructed with the length dimensions as in Fig. 4. The experiments were conducted in three different loops of different diameters (9.1 mm (1/2 in.), 15.74 mm (3/4 in.) and 19.86 mm (1 in.), respectively). For all different loop diameters, the steam drum, the condenser and the associated piping (the portion inside the rectangular box in Fig. 4) were the same. The steam drum was made up of 59 mm inside diameter (2.5 in. NB Sch. 80) pipe. The loop was designed for a pressure of 125 bar and temperature of 400 °C with 10 kW as maximum operating power. The vertical heater section was direct electrically heated. The steam so produced was condensed in the condenser and the condensate was returned to the steam drum. The loop was extensively instrumented to measure temperature, pressure, differential pressure, level, flow rate, void fraction and its distribution. The void fraction was measured using both neutron radiography (NRG) and conductance probe (CP) techniques. Further details of the loop are available in the report by Dubey et al. (2004).

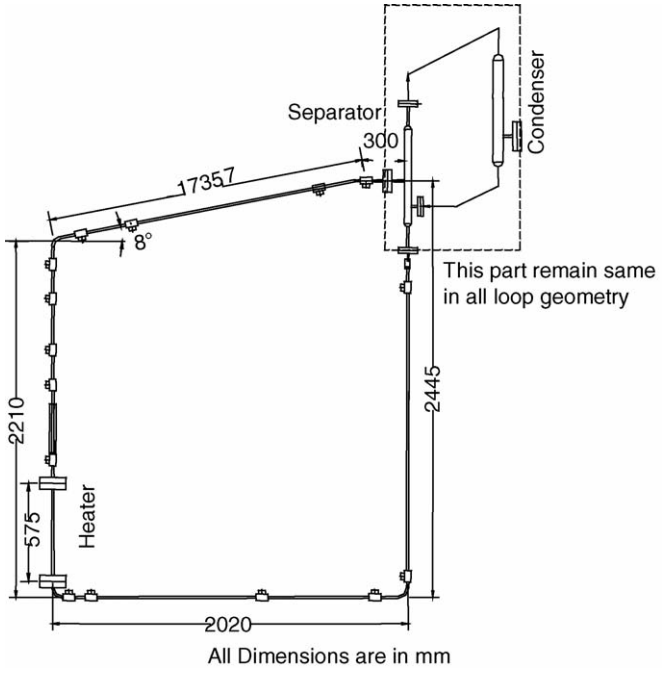

Fig. 4. Experimental loop.

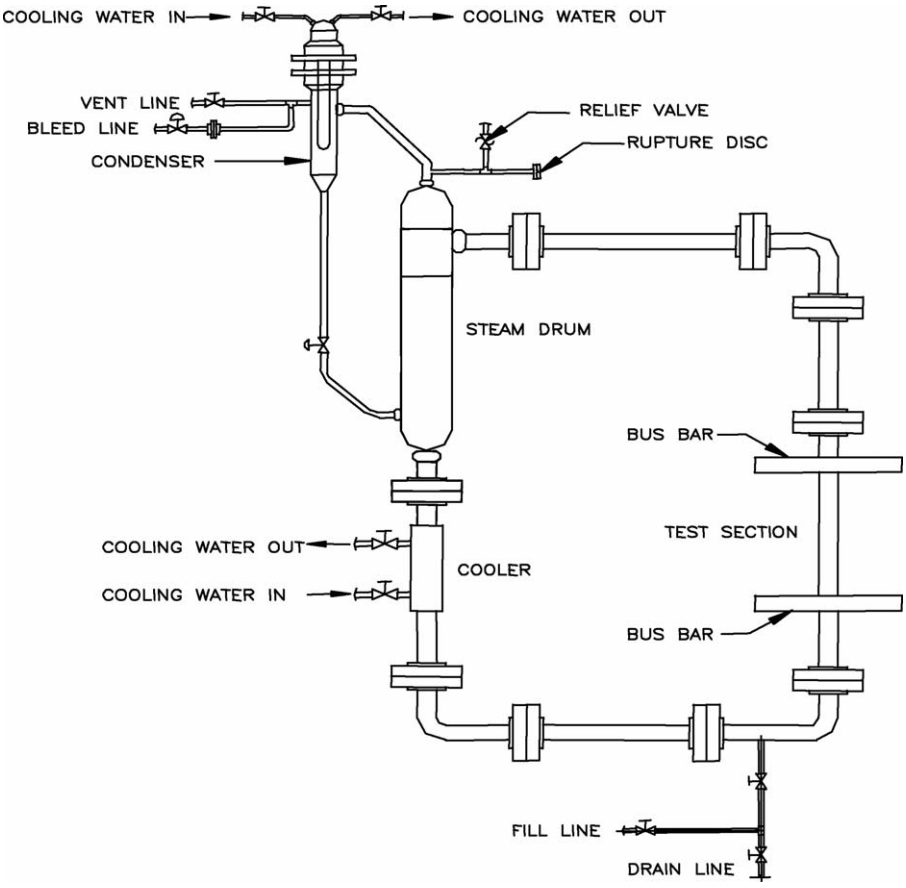

Fig. 5. High pressure natural circulation loop (HPNCL).

3.2. High pressure natural circulation loop

In addition, experimental data were generated in a 2 in. loop shown in Fig. 5. In this facility, experiments were carried out for power ranging from 0 kW to 40 kW and at pressure varying from 1 bar to 70 bar. The elevation of the primary loop is about 3.3 m and the length of heating section is about 1.25 m. The important design parameters of the loop are:

Design pressure = 114 bar
Design temperature = 315 °C

The inside diameter of different components of the loop are as given below:

Component	Pipe	I.D. (mm)
Test section	50 mm NB Sch. 40	52.5
Loop	50 mm NB Sch. 80	49.25
Steam drum	150 mm NB Sch. 120	139.7

Further details of the facility are available in Naveen et al. (2000).

3.3. Bettis natural circulation loop (Mendler et al.)

Fig. 6 shows the heated test section and natural circulation loop at Bettis Atomic Power Laboratory, Pittsburgh, USA. The main loop piping was fabricated from Sch. 80 type SS 304, and was in the shape of a vertical rectangle 4.4323 m (14.5 ft) high and 4.5466 m (15 ft) long. Heat was added uniformly to the lower part of the left vertical leg through an electrically heated rectangular channel test section. The test section was connected

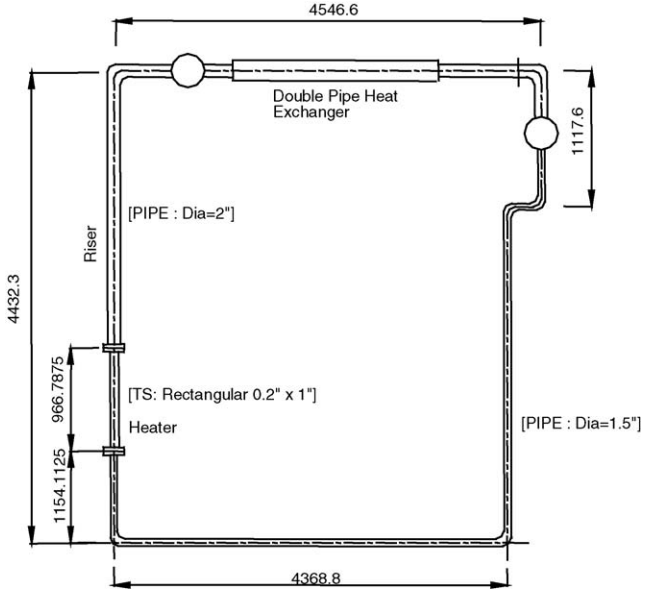

Fig. 6. Bettis natural circulation loop (Mendler et al., 1961).

to a riser made from 50.8 mm (2 in.) pipe; the other vertical leg is the down comer and was made from 38.1 mm (1.5 in.) pipe. The top horizontal leg consisted of a double pipe heat exchanger. The bottom horizontal leg contained an 8.636 mm (0.340 in.) diameter orifice and a preheater. The rectangular test sections were 685.8 mm (27 in.) long and 25.4 mm (1 in.) wide and were fabricated of SS 304. Here, 2.54 mm (0.1 in.) nominal spacing was taken as the natural circulation data were available for this dimension only. Further details of the loop can be obtained from Mendler et al. (1961).

4. Physical significance of the geometrical parameter (N_G)

The physical significance of the geometrical parameter, N_G, can be obtained from the loop pressure drop equation given below:

$$\Delta P_t = \frac{RW^2}{2\rho_r}$$

where the total hydraulic resistance, R is given by

$$R = \sum_{i=1}^{N} \left(\frac{f_i L_i}{D_i} + K_i \right) \frac{1}{A_i^2} \tag{19}$$

Hence

$$R = \sum_{i=1}^{N} \left(\frac{f L_{eff}}{D A^2} \right)_i$$

where $(L_{eff})_i = L_i + (L_{eq})_i$

Using Eq. (7), this can be rewritten as

$$R = \frac{L_t}{D_r} \frac{p}{Re_{ss}^b} \frac{1}{A_r^2} \left[\sum_{i=1}^{N_{sp}} \frac{(l_{eff})_i}{d_i^{1+b} a_i^{2-b}} + \bar{\phi}_{LO}^2 \sum_{i=N_{sp}}^{N_{he}} \frac{(l_{eff})_i}{d_i^{1+b} a_i^{2-b}} + \phi_{LO}^2 \sum_{i=N_{he}}^{N_t} \frac{(l_{eff})_i}{d_i^{1+b} a_i^{2-b}} \right], \quad \text{for steady state.}$$

From this, using Eq. (10) we can write

$$RA_r^2 = p \frac{N_G}{Re_{ss}^b} \quad \text{or} \quad K_{overall} = N_G \frac{p}{Re_{ss}^b} \tag{20}$$

where $K_{overall}$ is the effective loss coefficient for the entire loop or the friction number as suggested by Ishii and Kataoka (1984). Eq. (20) shows that the friction number can be expressed as the product of two terms, one of which is mainly flow dependent and the other is mainly geometry dependent (except the quality term in ϕ_{LO}^2). From this, N_G can be considered as the contribution of the loop geometry to the friction number. Again N_G depends upon the nature of the flow (i.e. laminar or turbulent) and the quality.

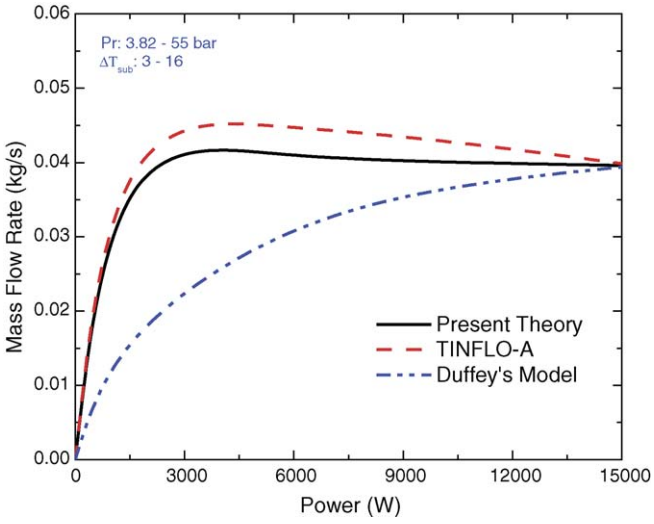

Fig. 7. Variation of flow rate for different pressures and different sub-cooling in 9.1 mm (1/2 in.) experimental loop.

5. Comparison of present theory with different theoretical models

5.1. Comparison of the correlation with codes

The mass flow rate calculated for the in-house experimental loop, using the present theory (Eq. (14)) has been compared with those calculated using computer code RELAP5/MOD 3.2 (Fletcher and Schultz, 1995), TINFLO-S (Nayak et al., 1998), TINFLO-A (Nayak et al., 1998), and Duffey's model (2000) under the same conditions.

Duffey's model is given by

$$(W_{ss}^3)_{Duffey} \approx \frac{2\rho_l^2 g Q H A_r^2 (\rho_l - \rho_g)}{h_{fg} \rho_l K_{overall}}$$

In TINFLO-S, TINFLO-A and present theory, Blassius friction factor correlation ($f = 0.316 Re^{-0.25}$) has been used. The results obtained are shown in Figs. 7 and 8.

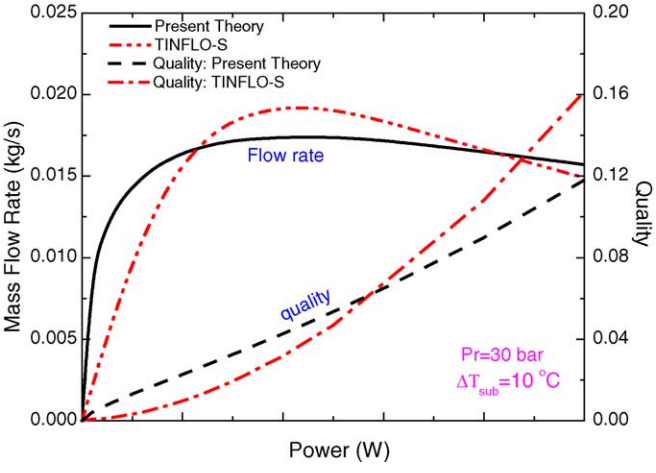

Fig. 8. Variation of flow rate for constant pressure and constant sub-cooling in 9.1 mm (1/2 in.) experimental loop.

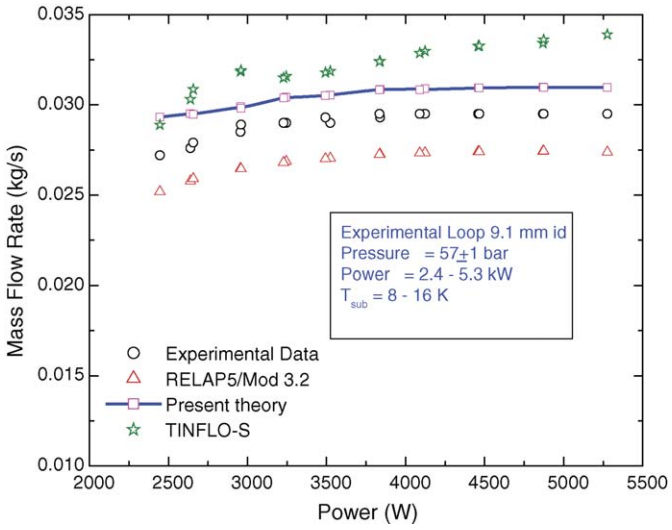

Fig. 9. Comparison of code prediction with experimental data.

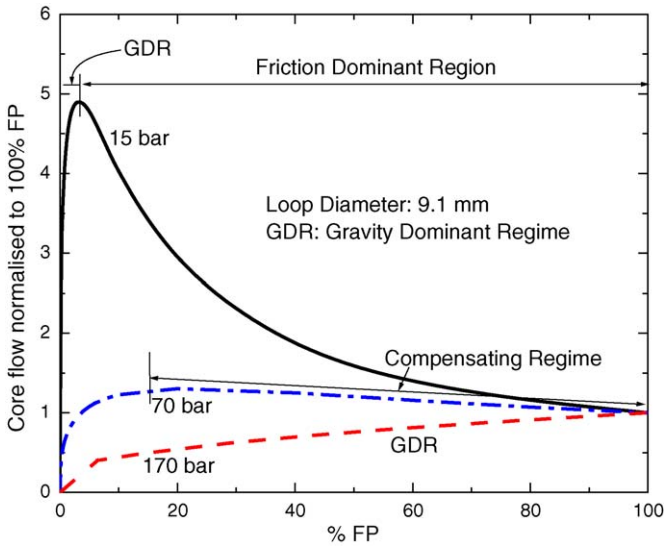

Fig. 10. Flow regime in two-phase loops.

These predictions are for the loop geometry given in Fig. 3 with inside diameter of 9.1 mm. It may be mentioned that the TINFLO (TINFLO-S and TINFLO-A) code is based on homogeneous model and used the same single-phase friction factor model used for developing the correlation and hence the predictions are closer to the generalized correlation. As seen from Fig. 7, present theory under predicts the mass flow rate by 0–12% as compared to TINFLO-A. Closer agreement could be obtained with other models for ϕ^2_{LO}. Fig. 8 shows the comparison of mass flow rates predicted by TINFLO-S and present theory. In the present theory the flow rates were calculated using Eq. (14) and β_{tp} is calculated by using Eq. (17a). TINFLO-S calculates the mass flow rate without any averaging of density (and hence β_{tp}). It can be seen that the averaging leads to close results above a quality of approximately 3% which is adequate for engineering calculations. Typical comparison of the measured flow rates with the predictions of the various codes is given in Fig. 9. RELAP5 code predictions are somewhat lower (5–8%) than the test data whereas predictions of Eq. (14) and TINFLO are, respectively, 5–7% and 5–13% higher.

5.2. Prediction of flow regimes in two-phase loops

Generally, dimensionless correlations are suffered with some disadvantages such as disguising the important parametric effects. Broadly, there are three flow regimes one can identify in a natural circulation loop, viz. gravity dominant regime, friction dominant regime and the compensating regime as shown in Fig. 10. In a natural circulation loop, the gravitational pressure drop (or the buoyancy pressure differential) is always the largest component of pressure drop and all other pressure drops (friction and local) must balance the buoyancy pressure differential at steady state. However, the natural circulation flow regimes are differentiated based on their change with quality (or power). In the gravity dominant regime, for a small change in quality there is a large change in the void fraction (see Fig. 11) and hence the density and buoyancy force. The increased buoyancy force is to be balanced by a corresponding increase in the frictional force which is possible only at a higher flow rate. As a result, the gravity dominant regime is characterized by an increase in the flow rate with power. At higher qualities and moderate pressures, the increase in void fraction with quality is marginal (Fig. 11) leading to almost constant buoyancy force. However, the continued conversion of high density water to low density steam due to increase in power requires that the mixture velocity must increase resulting in an increase in the frictional force and hence a decrease in flow rate. Thus, the friction dominant regime is characterized by a decrease in flow rate with increase in power. Between these two, there exists a compensating regime, where the flow rate remains practically unaffected with increase in power. However, the flow regimes depend strongly on the system pressure. In fact, at high pressures, only the gravity dominant regime may be observed if the power is low. The friction dominant regime shifts to low pressures with increase in loop diameter. This is clearly evident from Fig. 12a and b.

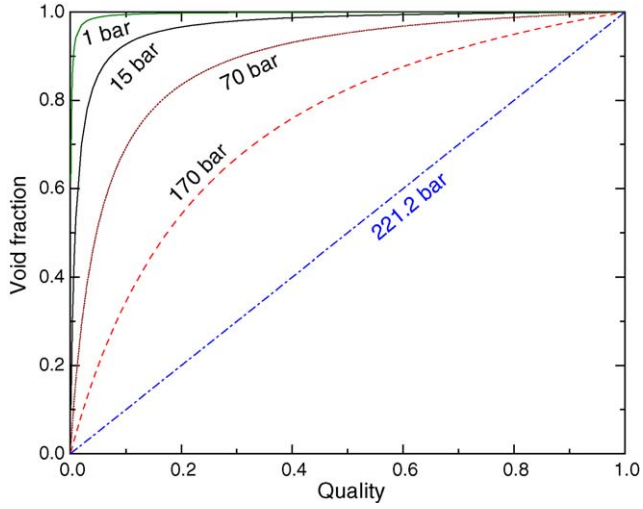

Fig. 11. Effect of pressure on void fraction.

Table 1
Range of parameters for the experimental data

Loops	D_h (mm)	L_t (m)	L_t/D_h	P (bar)	Loop height, H (m)	Quality, x	T_{sub} (°C)	Power, Q (W)	W_{ss} (kg/s)	Fluid
1/2 in. loop	9.1	8.58	840.42	1–58	2.445	0.008–0.239	0.1–29.0	298.1–5416	0.001–0.0305	Steam–water
3/4 in. loop	15.74	8.58	545.15	4–61	2.445	0.004–0.039	0.1–22.0	788–7425	0.044–0.1622	Steam–water
1 in. loop	19.86	8.58	432.06	8–59	2.445	0.005–0.011	0.1–13.0	1128–3668	0.108–0.2	Steam–water
BNCL (Mendler et al.)	8.47	17.8	2100	55–138	4.4323	0.082–0.693	8.0–64.0	8260–64,600	0.050–0.10	Steam–water
HPNCL (Naveen et al.)	52.5	13.4	254.38	2.0–46.0	3.350	0.007–0.017	0.3–2.1	20,000–36,500	0.9–1.8236	Steam–water

6. Testing of the steady-state correlation with experimental data

The steady-state data from five different two-phase natural circulation loops are compared with the theoretical correlation in Fig. 13. The experimental data is observed to be very close to the theoretical correlation (within an error bound of ±40%) for all the two-phase natural circulation loops confirming the validity of the correlations given in Eq. (16). The data of all the loops fall in the parameter range given in Table 1. Further, the steady-state mass flow rate has been calculated using present theory, RELAP5/MOD 3.2 and the in-house code TINFLO-A for the same experimental condition. Fig. 14 shows the comparison of mass flow rate ratio (experimental/theoretical) at different heater power. It is seen from Fig. 14, that the RELAP5 code is able to

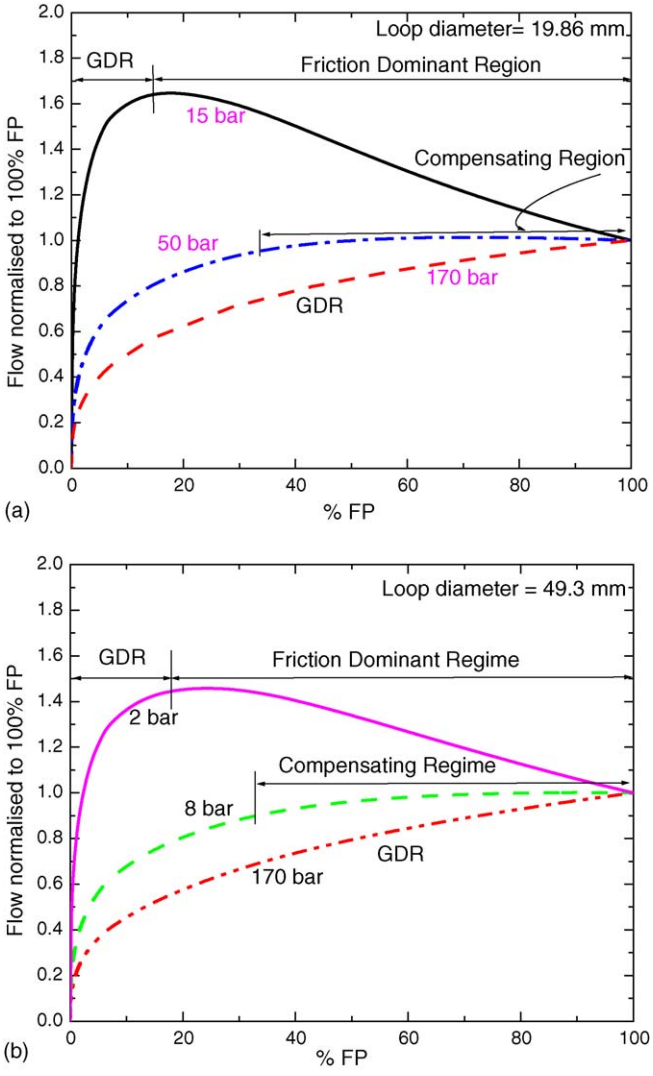

Fig. 12. Effect of loop diameter on flow regimes in two-phase natural circulation loops: (a) loop diameter = 19.86 mm and (b) loop diameter = 49.3 mm.

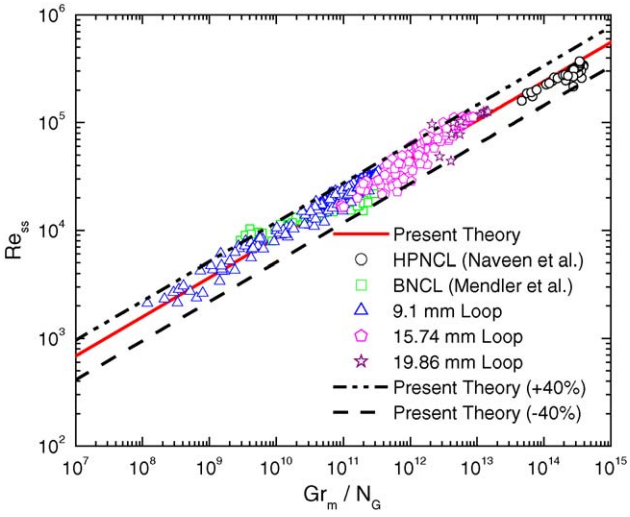

Fig. 13. Comparison of present theory and experimental results.

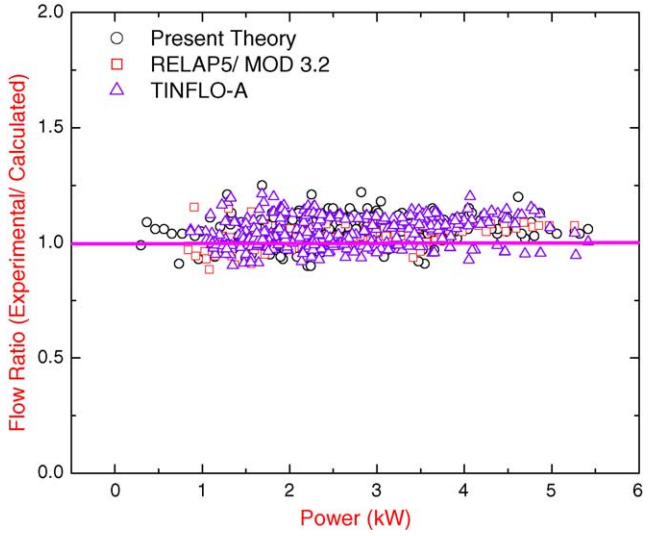

Fig. 14. Comparison of theoretical and experimental mass flow rate for 9.1 mm experimental loop.

Table 2
Comparison of various experimental data with present theory

Loops	Mean error (%)	Mean absolute error (%)	RMS error (%)	Standard deviation
1/2 in. (9.1 mm) loop	−11.38	13.34	19.02	15.25
3/4 in. (15.74 mm) loop	−6.40	16.29	19.32	18.28
1 in. (19.86 mm) loop	−1.33	17.71	25.43	26.36
HPNCL (Naveen et al.)	15.54	15.54	18.65	10.42
BNCL (Mendler et al.)	4.56	23.13	28.28	28.31

predict the experimental data with an error bound of ±15%. The prediction by TINFLO-A and present theory (i.e. Eq. (14)) falls within an error bound of ±21% and ±22%, respectively. This further reaffirms the validity of the present correlation.

7. Error analysis

An error analysis was carried out by standard statistical procedure. The error (e_i), mean error (e_m), mean of absolute error (e_{ma}), root mean square error (e_{rms}) and standard deviation (σ) are calculated as follows:

$$e_i = \left\{\frac{\xi_c - \xi_m}{\xi_m}\right\} \times 100, \qquad e_m = \frac{1}{N}\sum_{i=1}^{N} e_i,\ e_{ma} = \frac{1}{N}\sum_{i=1}^{N}|e_i|$$

$$e_{rms} = \left\{\frac{(\sum_{i=1}^{N} e_i^2)}{N}\right\}^{0.5} \quad \text{and} \quad \sigma = \left[\left\{\sum_{i=1}^{N}(e_m - e_i)^2\right\}\right]^{0.5}$$

where ξ_c and ξ_m are the calculated and measured quantities, respectively, and N the total number of data points. The results of error analysis are given in Table 2.

8. Conclusions

A generalized correlation for steady-state flow in two-phase natural circulation systems has been presented. For two-phase natural circulation systems, the steady-state behaviour can be simulated by preserving Gr_m/N_G same in the model and prototype. The given correlation has been tested with data from five different two-phase natural circulation loops. The experimental results are found to be in reasonable agreement with the proposed correlation.

References

Dubey, P., Rao, G.S.S.P., Pilkhwal, D.S., Vijayan, P.K., Saha, D., October 2004. Analysis of experimental data on two-phase natural circulation from the flow pattern transition instability studies facility at Apsara reactor. BARC/2004/E/031.

Duffey, R.B., 2000. Natural convection and natural circulation flow and limits in advanced reactor concepts, natural circulation data and methods for advanced water cooled nuclear power plant designs. In: Proceedings of Technical Committee Meeting, IAEA-TECDOC-1281, Vienna, pp. 49–65.

Fletcher, C.D., Schultz, R.R., 1995. RELAP5/MOD3 Code Manual Volume II: User's Guide and Input Requirements. Idaho National Engineering Laboratory, Idaho, USA.

Heisler, M.P., 1982. Nucl. Sci. Eng. 80, 347–359.

IAEA-TECDOC-1203, April 2001. Thermohydraulic relationships for advanced water cooled reactors. International Atomic Energy Agency, Chapter 5, pp. 109–162.

Ishii, M., Kataoka, I., 1984. Scaling laws for thermal–hydraulic system under single-phase and two-phase natural circulation. Nucl. Eng. Des. 81, 411–425.

Kocamustafaogullari, G., Ishii, M., 1987. Scaling of two-phase flow transients using reduced pressure system and simulant fluid. Nucl. Eng. Des. 104, 121–132.

Mendler, O.J., Rathbw, A.S., Van Huff, N.E., Weiss, A., 1961. Natural circulation tests with water at 800–2000 psia under non-boiling, local boiling and bulk boiling condition. J. Heat Transfer, 261–273.

Nahavandi, A.N., Castellana, F.S., Moradkhanian, E.N., 1979. Nucl. Sci. Eng. 72, 75–83.

Naveen, K., Rajalakshmi, R., Kulkarni, R.D., Sagar, T.V., Vijayan, P.K., Saha, D., February 2000. Experimental investigation in high pressure natural circulation loop. BARC/2000/E/002.

Nayak, A.K., Vijayan, P.K., Saha, D., Venkat Raj, V., Aritomi, M., 1998. Linear analysis of thermodynamic instabilities of the advanced heavy water reactor (AHWR). J. Nucl. Sci. Tech. 35, 768–778.

Reyes Jr., J.N., 1994. Scaling single-state variable catastrophe functions: an application to two-phase natural circulation loop. Nucl. Eng. Des. 151, 41–48.

Schwartzbeck, R.K., Kocamustafaogullari, G., 1989. Similarity requirements for two-phase flow pattern transitions. Nucl. Eng. Des. 116, 135–147.

Vijayan, P.K., Invited Talk, Misale, M., Mayinger, F. (Eds.), 1999. Proceedings of EUROTHERM SEMINAR no. 63 on Single and Two-Phase Natural Circulation. Genoa, Italy, 6–8 September 1999, pp. 3–16.

Vijayan, P.K., Nayak, A.K., Bade, M.H., Kumar, N., Saha, D., Sinha, R.K., 2000. Scaling of the steady state and stability behaviour of single- and two-phase natural circulation systems, natural circulation data and methods for advanced water cooled nuclear power plant designs. In: Proceedings of Technical Committee Meeting, IAEA-TECDOC-1281, Vienna, pp. 139–156.

Yadigaroglu, G., Zeller, M., 1994. Fluid-to-fluid scaling for gravity and flashing driven natural circulation loop. Nucl. Eng. Des. 151, 49–64.

Zuber, N., October 1980. Problems in modeling of small break LOCA. Report-NUREG-0724.